stable duplexes with ssRNA and unstable duplexes with ssDNA. In addition, oligonucleotides containing this analogue have increased stability against nuclease degradation, similar to a seven-membered bridge structure, maintaining high affinity with ssRNA. These investigations reveal that decreasing the ring size, which means increasing the ν_{max} value, increases binding affinity to ssRNA, and that a bulkier bridge structure produces greater nuclease resistance. These results suggest that the SuNA modification provides valuable information that can be applied to antisense technology. In addition, the SuNA-modified gapmer exhibited the degradation of complementary RNA through the RNase H mechanism, and further biological studies are in progress.

■ ASSOCIATED CONTENT

Supporting Information

Full experimental details, representative UV melting data, ^{1}H, ^{13}C, and ^{31}P spectra of all new compounds, and HPLC charts and MALDI-TOF-MS spectra of new oligonucleotides. This material is available free of charge via the Internet at http://pubs.acs.org.

■ AUTHOR INFORMATION

Corresponding Author

*E-mail: obika@phs.osaka-u.ac.jp.

Notes

The authors declare no competing financial interest.

■ REFERENCES

(1) Lee, R. G.; Crosby, J.; Baker, B. F.; Graham, M. J.; Crooke, R. M. *J. Cardiovasc. Transl. Res.* **2013**, *6*, 969.

(2) Reviews: (a) Kaur, H.; Babu, B. R.; Maiti, S. *Chem. Rev.* **2007**, *107*, 4672. (b) Obika, S.; Rahman, S. M. A.; Fujisaka, A.; Kawada, Y.; Baba, T.; Imanishi, T. *Heterocycles* **2010**, *81*, 1347.

(3) (a) Obika, S.; Nanbu, D.; Hari, Y.; Morio, K.; In, Y.; Ishida, T.; Imanishi, T. *Tetrahedron Lett.* **1997**, *38*, 8735. (b) Obika, S.; Nanbu, D.; Hari, Y.; Andoh, J.; Morio, K.; Doi, T.; Imanishi, T. *Tetrahedron Lett.* **1998**, *39*, 5401.

(4) (a) Singh, S. K.; Nielsen, P.; Koshkin, A. A.; Wengel, J. *Chem. Commun.* **1998**, 455. (b) Koshkin, A. A.; Singh, S. K.; Nielsen, P.; Rajwanshi, V. K.; Kumar, R.; Meldgaard, M.; Olsen, C. E.; Wengel, J. *Tetrahedron* **1998**, *54*, 3607.

(5) (a) Morita, K.; Hasegawa, C.; Kaneko, M.; Tsutsumi, S.; Sone, J.; Ishikawa, T.; Imanishi, T.; Koizumi, M. *Bioorg. Med. Chem. Lett.* **2002**, *12*, 73. (b) Morita, K.; Takagi, M.; Hasegawa, C.; Kaneko, M.; Tsutsumi, S.; Sone, J.; Ishikawa, T.; Imanishi, T.; Koizumi, M. *Bioorg. Med. Chem.* **2003**, *11*, 2211.

(6) (a) Miyashita, K.; Rahman, S. M. A.; Seki, S.; Obika, S.; Imanishi, T. *Chem. Commun.* **2007**, 3765. (b) Rahman, S. M. A.; Seki, S.; Obika, S.; Yoshikawa, H.; Miyashita, K.; Imanishi, T. *J. Am. Chem. Soc.* **2008**, *130*, 4886.

(7) (a) Hari, Y.; Obika, S.; Ohnishi, R.; Eguchi, K.; Osaki, T.; Ohishi, H.; Imanishi, T. *Bioorg. Med. Chem.* **2006**, *14*, 1029. (b) Mitsuoka, Y.; Kodama, T.; Ohnishi, R.; Hari, Y.; Imanishi, T.; Obika, S. *Nucleic Acids Res.* **2009**, *37*, 1225.

(8) Yahara, A.; Shrestha, A. R.; Yamamoto, T.; Hari, Y.; Osawa, T.; Yamaguchi, M.; Nishida, M.; Kodama, T.; Obika, S. *ChemBioChem* **2012**, *13*, 2513.

(9) Hari, Y.; Osawa, T.; Kotobuki, Y.; Shrestha, A. R.; Yahara, A.; Obika, S. *Bioorg. Med. Chem.* **2013**, *21*, 4405.

(10) Nishida, M.; Baba, T.; Kodama, T.; Yahara, A.; Imanishi, T.; Obika, S. *Chem. Commun.* **2010**, *46*, 5283.

(11) For other nucleic acids bridged between the 2′- and 4′-positions, see: (a) Kumar, R.; Singh, S. K.; Koshkin, A. A.; Rajwanshi, V. K.; Meldgaard, M.; Wengel, J. *Bioorg. Med. Chem. Lett.* **1998**, *8*, 2219. (b) Singh, S. K.; Kumar, R.; Wengel, J. *J. Org. Chem.* **1998**, *63*, 10035. (c) Varghese, O. P.; Barman, J.; Pathmasiri, W.; Plashkevych, O.; Honcharenko, D.; Chattopadhyaya, J. *J. Am. Chem. Soc.* **2006**, *128*, 15173. (d) Albæk, N.; Petersen, M.; Nielsen, P. *J. Org. Chem.* **2006**, *71*, 7731. (e) Srivastava, P.; Barman, J.; Pathmasiri, W.; Plashkevych, O.; Wenska, M.; Chattopadhyaya, J. *J. Am. Chem. Soc.* **2007**, *129*, 8362. (f) Seth, P. P.; Siwkowski, A.; Allerson, C. R.; Vasquez, G.; Lee, S.; Prakash, T. P.; Wancewicz, E. V.; Witchell, D.; Swayze, E. E. *J. Med. Chem.* **2009**, *52*, 10. (g) Zhou, C.; Liu, Y.; Andaloussi, M.; Badgujar, N.; Plashkevych, O.; Chattopadhyaya, J. *J. Org. Chem.* **2009**, *74*, 118. (h) Seth, P. P.; Vasquez, G.; Allerson, C. A.; Berdeja, A.; Gaus, H.; Kinberger, G. A.; Prakash, T. P.; Migawa, M. T.; Bhat, B.; Swayze, E. E. *J. Org. Chem.* **2010**, *75*, 1569. (i) Seth, P. P.; Allerson, C. R.; Berdeja, A.; Siwkowski, A.; Pallan, P. S.; Gaus, H.; Prakash, T. P.; Watt, A. T.; Egli, M.; Swayze, E. E. *J. Am. Chem. Soc.* **2010**, *132*, 14942. (j) Shrestha, A. R.; Hari, Y.; Yahara, A.; Osawa, T.; Obika, S. *J. Org. Chem.* **2011**, *76*, 9891. (k) Hari, Y.; Morikawa, T.; Osawa, T.; Obika, S. *Org. Lett.* **2013**, *15*, 3702. (l) Morihiro, K.; Kodama, T.; Kentefu; Moai, Y.; Veedu, R. N.; Obika, S. *Angew. Chem., Int. Ed.* **2013**, *52*, 5074.

(12) Reviews: (a) Supuran, C. T.; Casini, A.; Scozzafava, A. *Med. Res. Rev.* **2003**, *23*, 535. (b) Kamal, A.; Faazil, S.; Malik, M. S. *Expert Opin. Ther. Patents* **2014**, *24*, 339. (c) Carta, F.; Supuran, C. T.; Scozzafava, A. *Future Med. Chem.* **2014**, *6*, 1149.

(13) Waga, T.; Nishizaki, T.; Miyakawa, I.; Ohrui, H.; Meguro, H. *Biosci. Biotechnol. Biochem.* **1993**, *57*, 1433.

(14) Nishiguchi, A.; Maeda, K.; Miki, S. *Synthesis* **2006**, 4131.

(15) CCDC 1018300 contains the supplementary crystallographic data for this paper. These data can be obtained free of charge from the Cambridge Crystallographic Data Centre via http://www.ccdc.cam.ac.uk/data_request/cif.

(16) Pallan, P. S.; Allerson, C. R.; Berdeja, A.; Seth, P. P.; Swayze, E. E.; Prakash, T. P.; Egli, M. *Chem. Commun.* **2012**, *48*, 8195.

(17) Lima, W.; Wu, H.; Crooke, S. T. In *Antisense Drug Technology: Principles, Strategies and Applications*, 2nd ed.; Crooke, S. T., Ed.; CRC Press: Boca Raton, 2007; pp 47–74.

(18) Bennett, C. F. In *Antisense Drug Technology: Principles, Strategies and Applications*, 2nd ed.; Crooke, S. T., Ed.; CRC Press: Boca Raton, 2007; pp 273 –304.

Molecules **2014**, *19*, 5109-5118; doi:10.3390/molecules19045109

OPEN ACCESS

molecules

ISSN 1420-3049

www.mdpi.com/journal/molecules

Communication

C5-Azobenzene-substituted 2'-Deoxyuridine-containing Oligodeoxynucleotides for Photo-Switching Hybridization

Shohei Mori [1], Kunihiko Morihiro [1,2,*] and Satoshi Obika [1,2,*]

[1] Graduate School of Pharmaceutical Sciences, Osaka University, 1-6 Yamadaoka, Suita, Osaka 565-0871, Japan; E-Mail: mori-s@phs.osaka-u.ac.jp

[2] National Institute of Biomedical Innovation (NIBIO), 7-6-8 Saito-Asagi, Osaka 567-0085, Japan

* Authors to whom correspondence should be addressed; E-Mails: morihiro@phs.osaka-u.ac.jp (K.M.); obika@phs.osaka-u.ac.jp (S.O.); Tel.: +81-6-6879-8202 (K.M.); +81-6-6879-8200 (S.O.); Fax: +81-6-6879-8204 (K.M & S.O.).

Received: 3 March 2014; in revised form: 15 April 2014 / Accepted: 17 April 2014 / Published: 22 April 2014

Abstract: A new photoisomeric nucleoside **dU^{Az}** bearing an azobenzene group at the C5-position of 2'-deoxyuridine was designed and synthesized. Photoisomerization of **dU^{Az}** in oligodeoxynucleotides can be achieved rapidly and selectively with 365 nm (forward) and 450 nm (backward) irradiation. Thermal denaturation experiments revealed that **dU^{Az}** stabilized the duplex in the *cis*-form and destabilized it in the *trans*-form with mismatch discrimination ability comparable to thymidine. These results indicate that **dU^{Az}** could be a powerful material for reversibly manipulating nucleic acid hybridization with spatiotemporal control.

Keywords: azobenzene; molecular switch; nucleoside; oligonucleotide; photochromism

---

1. Introduction

Regulation of nucleic acid hybridization by some external stimuli is a rewarding challenge due to its potential to control gene expression flow from DNA to protein at a predetermined place and time. This technique could allow for spatiotemporal controllable pharmacotherapy based on nucleic acid agents. The regulation of nucleic acid hybridization is also important in the field of nanotechnology, such as in the construction of DNA-origami [1–3]. Modified oligonucleotides (ONs) that can reversibly alter the hybridization ability by noninvasive external stimuli are therefore necessary. The most promising

external stimulus is light, due to the possibility of accurately controlling the location, dosage and time of the irradiation. For example, Asanuma *et al.* have reported reversible photoregulation of DNA duplex formation via installation of azobenzene moieties on ONs [4,5]. Azobenzene and its derivatives are commonly adopted due to their rapid photoisomerization and drastic changes in geometry and dipole moment [6,7].

In this study, we describe a new type of azobenzene-modified nucleoside that reversibly changes its properties upon photoisomerization by ultraviolet (365 nm) or visible light (450 nm). There are several positions to attach a photochromic moiety to a nucleoside, and we have selected the C5 position of 2'-deoxyuridine (**dU^{Az}**, Figure 1) [8]. It is predicted that the azobenzene moiety of **dU^{Az}** is projected into the major groove of the double helix via a rigid ethynyl linker. We assumed that the duplexes containing *trans*-**dU^{Az}** would be destabilized because the hydrophobic azobenzene moiety extends to the outside of the groove [9] which surrounded by a highly polar aqueous phase, and interferes with hydration and the formation of interstrand cation bridges to stabilize the duplexes [10,11]. Meanwhile, *cis*-**dU^{Az}**-modification would not affect the duplex stability due to compact conformation of the azobenzene moiety. In other words, the affinity of ONs containing **dU^{Az}** for complementary single-stranded DNA or RNA may be reversibly changed, triggered by light.

Figure 1. Photoisomeric nucleoside used in this study.

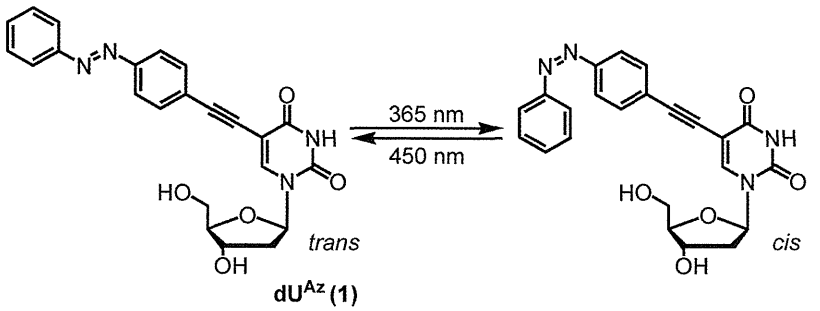

2. Results and Discussion

2.1. Synthesis of dU^{Az} Phosphoramidite and dU^{Az}-Modified Oligodeoxynucleotides

The synthetic route of **dU^{Az}** phosphoramidite is outlined in Scheme 1. **dU^{Az}** nucleoside **1** was synthesized from the corresponding 2'-deoxy-5-iodouridine (**2**) through a palladium-catalyzed cross-coupling reaction [12] with 4-ethynylazobenzene **3** [13]. Tritylation at the primary hydroxyl group of **1** with DMTrCl and phosphitylation at the secondary hydroxyl group yielded phosphoramidite **5**. The amidite **5** was incorporated into the oligodeoxynucleotide using conventional solid-phase phosphoramidite synthesis and purified by reverse-phase HPLC (29% yield). The ON sequences used in this study are shown in Table 1.

Scheme 1. Route for the synthesis of **dU^{Az}** phosphoramidite.

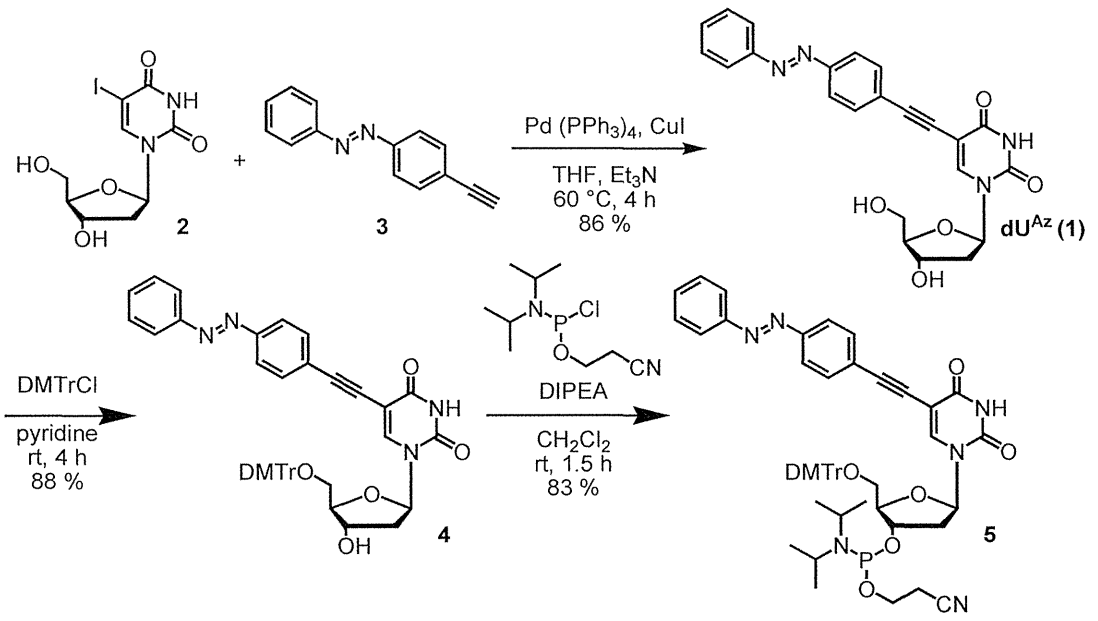

Table 1. The oligonucleotides used in this study.

ON	Sequence	
6	5'-d(GCGTTTTTTGCT)-3'	control DNA
7	5'-d(GCGTT**U^{Az}**TTTGCT)-3'	**dU^{Az}**-modified DNA
8	5'-d(AGCAAAAAACGC)-3'	full match DNA
9	5'-d(AGCAAATAACGC)-3'	mismatch DNA (T)
10	5'-d(AGCAAACAACGC)-3'	mismatch DNA (C)
11	5'-d(AGCAAAGAACGC)-3'	mismatch DNA (G)
12	5'-r(AGCAAAAAACGC)-3'	full match RNA
13	5'-r(AGCAAAUAACGC)-3'	mismatch RNA (U)
14	5'-r(AGCAAACAACGC)-3'	mismatch RNA (C)
15	5'-r(AGCAAAGAACGC)-3'	mismatch RNA (G)

2.2. Photoisomerization Property of dU^{Az}

We initially investigated the efficiency of the **dU^{Az}** *cis-trans* photoisomerization property in ON by UV spectra and HPLC analysis. UV spectra of *trans/cis* ON **7**, showed that photoisomerization of *trans*-**dU^{Az}** to *cis*-**dU^{Az}** decreased absorbance at 365 nm and increased absorbance at 310 nm and 450 nm (Figure 2a). The λ_{max} of *cis*-form (340 nm) was blue-shifted compared to that of the *trans*-form (365 nm), as was the case with previous reports [6,7,14]. The *trans*-form **dU^{Az}** was photoisomerized to the *cis*-form by a 10-second irradiation of 365 nm monochromic light with 60% conversion, as determined by the HPLC peak areas (Figure 2b). In addition, subsequent 10-second irradiation of 450 nm yielded the *trans* form isomer with 80%. The HPLC analysis showed no side products from the reactions.

Even when the photoirradiation was repeated three times, the efficiency of the **dU^{Az}** *cis-trans* photoisomerization was not attenuated (Figure 2c). It can therefore be concluded that **dU^{Az}** has a rapid

and highly efficient *cis-trans* photoisomerization property and the potential to work as a photo-switch for various biomolecules.

Figure 2. Photoisomerization properties of $\mathbf{dU^{Az}}$ in oligodeoxynucleotide. (**a**) Absorbance spectra of *trans-* (black line) and *cis-* (red line) ON 7. (**b**) HPLC analysis of the photoisomerization of ON 7; (i) Before irradiation; (ii) after 365 nm irradiation for 10 s; (iii) subsequent irradiation at 450 nm, 10 s. (**c**) Repetitive photoisomerization of ON 7 induced by alternative light irradiation at 365 nm and 450 nm. The percentages of *trans-* (black line) and *cis-* (red line) ON 7 obtained from the HPLC peak areas are shown. Conditions: ON 7 (4.0 μM), NaCl (100mM) in sodium phosphate buffer (10 mM, pH 7.0) was irradiated at room temperature.

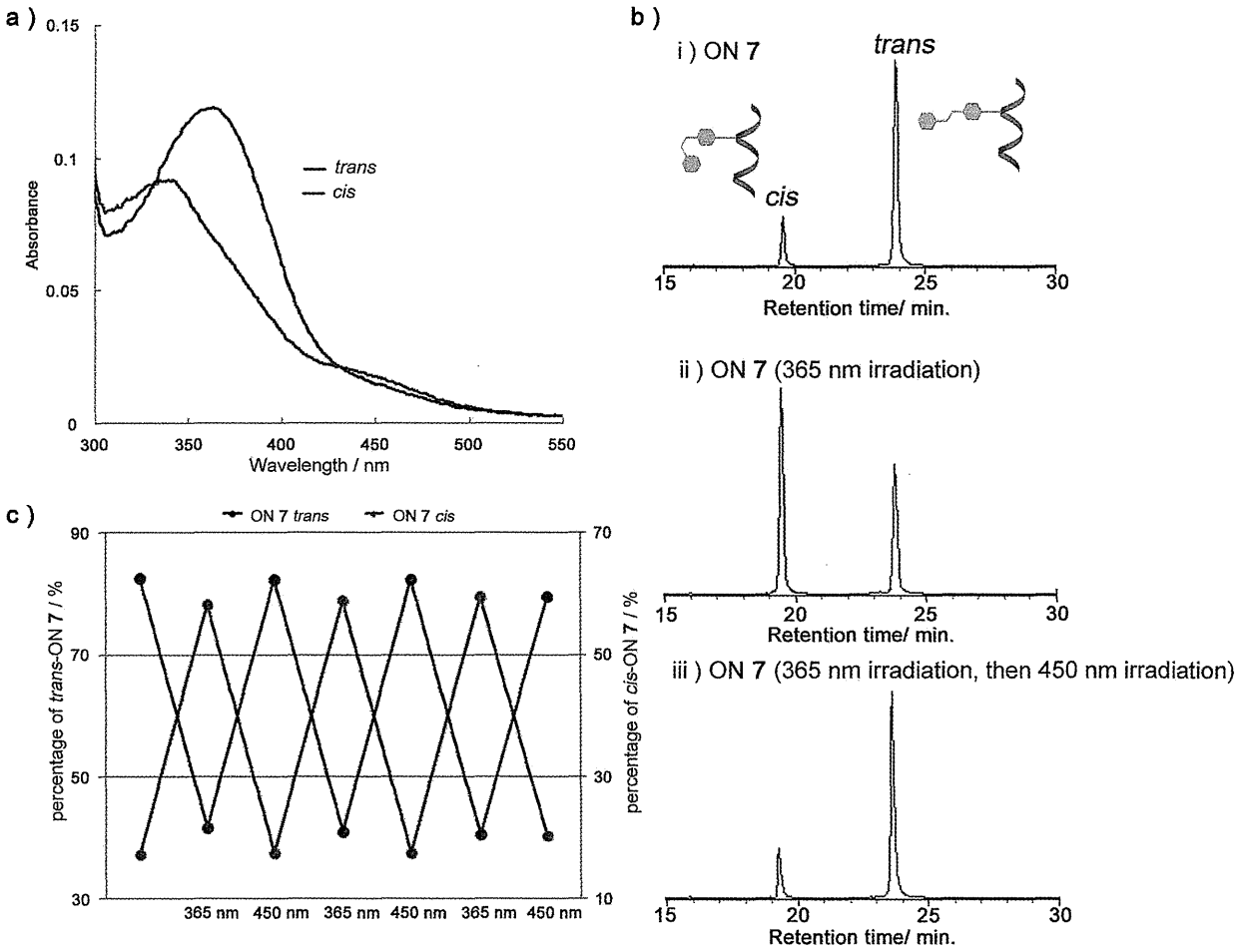

We investigated the differences in the thermal stability of 12-bp duplexes containing $\mathbf{dU^{Az}}$ in the *trans-* and *cis*-forms by monitoring the melting temperature (T_m) following the way of azobenzene-modified nucleoside containing ONs (Table 2) [15,16]. DNA duplex **7**/**8** showed a modest T_m difference (ΔT_m) between the *trans-* and *cis*-forms, namely, the T_m value of the *cis*-form was 2 °C higher than that of the *trans*-form. On the other hand, the ON **7**/RNA **12** duplex showed a larger T_m difference. The T_m value of the *cis*-form was 5 °C higher than that of the *trans*-form. It is noteworthy that the *cis*-ON **7**/RNA **12** duplex showed a T_m value comparable to that of natural DNA **6**/RNA **12**

duplex. According to past studies, the *cis*-form photochromic moieties generically destabilize the duplex because of its interference with the vicinity bases stacking interaction [4,5,17–19].In this study, ON containing **dU**^{Az} showed a higher hybridization ability when **dU**^{Az} is *cis*-form rather than *trans*-form, unlike ONs containing the exiting photochromic nucleoside. Brown *et al.* have reported that hydrophobic buta-1,3-diynyl anthracene in ON leads to significant destabilization of the duplex, probably because the aromatic moiety is exposed to the aqueous environment [9]. The azobenzene moiety of *trans*-**dU**^{Az} also would extend to the outside of the major groove, a highly polar aqueous phase. This may have an impact on the groove hydration and the formation of interstrand cation bridges, and lead to destabilization of the duplex containing *trans*-**dU**^{Az}.

Table 2. UV-melting points of 12-bp duplexes. [a]

Duplex	T_m [°C]		ΔT_m [°C] [b]
	trans [c]	*cis* [d]	($T_{m\ cis}$ - $T_{m\ trans}$)
6/8	52		-
7/8	47	49	2
6/12	47		
7/12	42	47	5

[a] All T_m values for the duplexes (4.0 μM) were determined in 10 mM sodium phosphate buffer (pH 7.0) containing 100 mM NaCl. The T_m values given are the average of at least three data points; [b] The change in the T_m value induced by the *cis-trans* photoisomerization; [c] The percentage of *trans* isomer was *ca.* 80%; [d] The percentage of *cis* isomer was *ca.* 60%.

Finally, we investigated the mismatch discrimination ability of ON containing **dU**^{Az}. The T_m values of mismatched DNA duplexes containing **dU**^{Az} were found to be 14 or 15 °C lower than that of ON7/DNA**8** in both *trans*- and *cis*-form (Table 3). Toward complementary ssRNA, ON containing **dU**^{Az} could also discriminate mismatched bases comparable to ON7 (Table S1 in Supplementary Material). These results indicate that the mismatch discrimination ability of ON containing *trans*-/*cis*-**dU**^{Az} is not spoiled by the C5-substituted-azobenzene moiety of **dU**^{Az}.

Table 3. UV-melting points of DNA duplexes with a mismatched base pair. [a]

Duplex	Base pair	T_m [°C]		ΔT_m [°C] [b]	
		trans [c]	*cis* [d]	*trans* [c]	*cis* [d]
6/9	T:T	40		−12	
6/10	T:C	37		−15	
6/11	T:G	41		−11	
7/9	**U**^{Az}:T	33	35	−14	−14
7/10	**U**^{Az}:C	33	34	−14	−15
7/11	**U**^{Az}:G	33	35	−14	−14

[a] All T_m values for the duplexes (4.0 μM) were determined in 10 mM sodium phosphate buffer (pH 7.0) containing 100 mM NaCl. The T_m values given are the average of at least three data points; [b] ΔT_m values are calculated relative to the T_m values of matched DNA **6**/DNA **8** (52 °C) or ON 7/DNA **8** (47 °C for *trans* and 49 °C for *cis*) duplexes.; [c] The percentage of *trans* isomer was *ca.* 80%; [d] The percentage of *cis* isomer was *ca.* 60%.

We achieved synthesis of the photoisomeric nucleoside, $\mathbf{dU^{Az}}$, for which the hybridization can be controlled by using different wavelengths of light. The ΔT_m value between the *trans*- and *cis*-form is more remarkable in the DNA/RNA duplex than the DNA duplex. Although $\mathbf{dU^{Az}}$ photoisomerization induced modest T_m differences, the modification of ONs with multiple $\mathbf{dU^{Az}}$ units or the introduction of substituents to the azobenzene moiety [20] could enhance the ΔT_m value between the *trans*- and *cis*-forms. Our strategy indicated the possibility of photo-switches based on $\mathbf{dU^{Az}}$-modified ONs for the development of unique molecular machines and the control of various biological phenomena.

3. Experimental

3.1. General

Reagents and solvents were purchased from commercial suppliers and were used without purification unless otherwise specified. All experiments involving air and/or moisture-sensitive compounds were carried out under N_2 or Ar atmosphere. All reactions were monitored with analytical TLC (Merck Kieselgel 60 F254). Column chromatography was carried out with a Fuji Silysia FL-100D. Physical data were measured as follows: NMR spectra were recorded on a JEOL JNM-ECS-500 spectrometer in $CDCl_3$ or DMSO-d_6 as the solvent with tetramethylsilane as an internal standard. IR spectra were recorded on a JASCO FT/IR-4200 spectrometer. Optical rotations were recorded on a JASCO P-2200 instrument. FAB mass spectra were measured on a JEOL JMS-700 mass spectrometer.

3.2. Preparation of 5-(4-Phenyldiazenylphenyl)ethynyl-2'-deoxyuridine (**1**)

Under an argon atmosphere, 4-ethynylazobenzene (**3** [13], 1.06 g, 5.12 mmol), $Pd(PPh_3)_4$ (592 mg, 0.512 mmol), and CuI (113 mg,0.512 mmol) was dissolved in dry DMF (50 mL). Then, Et_3N (3.6 mL) and 2'-deoxy-5-iodouridine (**2**, 1.81 g, 5.12 mmol) were added. The reaction mixture was stirred at 60 °C for 4 h. The resultant mixture was filtered over Celite. The filtrate was concentrated *in vacuo*. The residue was purified by silica gel column chromatography and eluted with $CHCl_3$/MeOH (20:1), to give compound **1** (1.80 g, 81%) as a light-orange powder: M.p. 208–210 °C; IR (KBr): ν 3439 (NH, OH), 1617 (C=O), 1289 (N=N) cm^{-1}; $[\alpha]_D^{24}$ −3.7 (c 1.00, DMSO); ^{1}H-NMR (500 MHz, DMSO-d_6): δ 11.7 (1H, brs, NH), 8.47 (1H, s, H-6), 7.94–7.90 (4H , m), 7.69–7.57 (5H, m), 6.14 (1H, t, J = 6.5 Hz, *H*-1'), 5.27 (1H, d, J = 4.0 Hz, H-3'), 5.20 (1H, t, J = 5.0 Hz, C-H4'), 4.30–4.26 (1H, m, OH), 3.82 (1H, m, OH), 3.71–3.58 (2H, m, H-5'), 2.21–2.17 (2H, m, H.2'); ^{13}C-NMR (125 MHz, DMSO-d_6): δ 161.3, 151.9, 151.0, 149.4, 132.2, 131.8, 129.5, 125.4, 122.9, 122.6, 97.8, 91.5, 87.6, 85.6, 84.9, 69.8, 60.8, 40.2; FAB-LRMS m/z = 433 (MH^+); FAB-HRMS calcd for $C_{23}H_{21}N_4O_5$ 433.1506, found 433.1524.

3.3. Preparation of 5'-O-(4,4'-Dimethoxytrityl)-5-(4-phenyldiazenylphenyl)ethynyl-2'-deoxyuridine (**4**)

To a solution of compound **1** (141 mg, 0.324 mmol) in dry pyridine (3 mL) was added DMTrCl (131 mg, 0.389 mmol) at room temperature, and the reaction mixture was stirred for 4 h. The reaction was quenched by the addition of MeOH with 10 min stirring. The solvent was removed *in vacuo*, and the residue was partitioned between $CHCl_3$ and H_2O. The separated organic layer was washed with H_2O, followed by brine. The organic layer was dried (Na_2SO_4) and concentrated in vacuo. The residue was purified by silica gel column chromatography and eluted with $CHCl_3$/MeOH (20:1 with 0.5%

Et_3N) to give Compound **4** (239 mg, 88%) as an orange foam: IR (KBr): *v* 3437, 3410(NH, OH), 1701 (C=O), 1272 (N=N) cm^{-1}; $[\alpha]_D^{24}$ 36.2 (c 1.00, $CHCl_3$); ^{1}H-NMR (500 MHz, $CDCl_3$): δ 8.51 (1H, brs, NH), 8.29 (1H, s, H-6), 7.90 (2H, d, J = 7.5 Hz), 7.70 (2H, d, J = 8.5 Hz), 7.52–7.45 (5H, m), 7.37–7.28 (6H, m), 7.16 (1H, dd, J = 6.5 and 1.0 Hz), 7.10 (2H, d, J = 8.0 Hz), 6.82–6.79 (4H, m) 6.38 (1H, dd, J = 7.5, 6.5 Hz, H-1'), 4.60–4.59 (1H, m, H-3'), 4.14–4.13 (1H, m, H-4'), 3.70 (3H, s,OMe), 3.69 (3H, s, OMe), 3.50 (1H, dd, J = 8.0 and 3.0 Hz, H-5'), 3.34 (1H, dd, J = 8.0 and 3.0 Hz, H-5'), 2.57–2.53 (1H, m, H-2'), 2.40–2.34 (1H, m, H-2'), 2.09 (1H, brs, OH); ^{13}C-NMR (125 MHz, $CDCl_3$): δ 158.6, 152.6, 151.7, 148.8, 144.3, 135.4, 132.4, 131.3, 129.9, 129.1, 128.1, 127.9, 127.1, 125.1, 122.9, 122.5, 113.4, 100.4, 93.6, 87.2, 86.7, 85.9, 82.2, 72.4, 63.3, 55.2, 41.7; FAB-LRMS *m/z* = 757 (MNa^+); FAB-HRMS calcd for $C_{44}H_{38}N_4O_7Na$ 757.2633, found 757.2633.

3.4. Preparation of 3-O-{2-Cyanoethyl(diisopropylamino)phosphino}-5'-O-(4,4'-Dimethoxytrityl)-5-(4-phenyldiazenylphenyl)ethynyl-2'-deoxyuridine (**5**)

To a solution of compound **4** (188 mg, 0.26 mmol) in dry MeCN (5 mL) was added *N,N*-diisopropylamine (0.13 mL,0.76 mmol) and 2-cyanoethyl-*N,N'*-diisopropylchlorophosphoramidite (0.09 mL, 0.40mmol) at room temperature, and the reaction mixture was stirred for 1.5 h. The resultant mixture was partitioned between AcOEt and H_2O. The separated organic layer was washed with saturated aqueous $NaHCO_3$, followed by brine. The organic layer was dried (Na_2SO_4) and concentrated in vacuo. The residue was purified by silica gel column chromatography and eluted with $CHCl_3$/MeOH (20:1 with 0.5% Et_3N), to give a 17:3 diastereomeric mixture of **5** (324 mg, 82%) as an orange foam: IR (KBr): *v* 3610 (NH), 1699 (C=O), 1272 (N=N) cm^{-1}; $[\alpha]_D^{24}$ 32.5 (c 1.00, $CHCl_3$); ^{1}H-NMR (500 MHz, $CDCl_3$): δ 9.08 (1H, brs, NH), 8.35 (0.85H, s, H-6), 8.30 (0.15H, s, H-6), 7.89 (2H, d, J = 7.5 Hz), 7.67 (2H, d, J = 8.5 Hz), 7.55–7.04 (14H, m), , 6.67–6.75 (4H, m), , 6.35 (1H, dd, J = 7.5, 6.0 Hz, H-1'), 4.68–4.61 (1H, m, H-3'), 4.26 (1H,m, H-4'), 3.70 (3H, s, OMe), 3.69 (3H, s, OMe), 3.67–3.53 (5H, m, CH_2CH_2CN, H-5'), 3.31 (1H, dd, J = 8.5, 2.5 Hz, H-5'), 2.65–2.56 (1H, m, H-2'), 2.47–2.36 (3H, m, H-2', $((CH_3)_2CH)_2N$), 1.18 (12H, d, J = 6.5 Hz, $((CH_3)_2CH)_2N$); ^{13}C-NMR (125 MHz, $CDCl_3$): δ 161.2, 158.5(9), 158.5(6), 152.6, 151.5, 149.1, 144.35, 142.5, 135.4, 132.3, 132.0, 131.1, 130.0 (d, J (C, P) = 6.0 Hz), 129.1, 128.7, 128.0, 127.9 ,127.0, 125.1, 122.8, 122.4, 120.5, 117.3, 113.3, 100.3, 93.4, 86.3 (d, J (C, P) = 3.5 Hz), 85.9, 82.4, 77.3, 77.0, 76.8, 73.4, 73.2, 63.0, 58.2, 58.1, 55.1, 43.2 (d, J (C, P) = 13.0 Hz), 40.8 (d, J (C, P) = 5.0 Hz), 25.6, 24.5(9), 24.5(3), 24.4(8), 20.2 (d, J (C, P) = 7.0 Hz); ^{31}P-NMR (200 MHz, $CDCl_3$): δ 149.09, 148.66; FAB-LRMS *m/z* = 957 (MNa^+); FAB-HRMS calcd for $C_{53}H_{55}N_6O_8PNa$ 957.3711, found 957.3711.

3.5. Synthesis of dU^{Az}*-Modified Oligodeoxynucleotides*

Solid-phase oligonucleotide synthesis was performed on an nS-8 Oligonucleotides Synthesizer (GeneDesign, Inc., Osaka, Japan) using commercially available reagents and phosphoramidites with 5-(bis-3, 5-trifluoromethylphenyl)-1*H*-tetrazole (0.25 M concentration in acetonitrile) as the activator. dU^{Az} phosphoramidite was chemically synthesized as described above. All of the reagents were assembled, and the oligonucleotides were synthesized according to the standard synthesis cycle (trityl on mode). Cleavage from the solid support and deprotection were accomplished with concentrated ammonium hydroxide solution at 55 °C for 12 h. The crude oligonucleotides were purified with

Sep-Pak Plus C18 cartridges (Waters) followed by RP-HPLC on a XBridge™ OST C18 Column, 2.5 μm, 10 × 50 mm (Waters) using MeCN in 0.1 M triethylammonium acetate buffer (pH 7.0). The purified oligonucleotides were quantified by UV absorbance at 260 nm and confirmed by MALDI-TOF mass spectrometry (Table 4).

Table 4. Yields and MALDI-TOF MS data of **dU^{Az}**-modified oligonucleotide.

Oligodeoxynucleotide		Yield	MALDI-TOF MS	
			Calcd. [M-H]$^-$	found [M-H]$^-$
5'-d(GCGTTU^{Az}TTTGCT)-3'	7	29%	3822.6	3822.4

3.6. UV Melting Experiments

Melting temperatures (T_m) were determined by measuring the change in absorbance at 260 nm as a function of temperature using a Shimadzu UV-Vis Spectrophotometer UV-1650PC equipped with a T_m analysis accessory TMSPC-8. Equimolecular amounts of the target DNA/RNA and oligonucleotides were dissolved in 10 mM sodium phosphate buffer (pH 7.0) containing 100 mM NaCl to give a final strand concentration of 4.0 μM. The melting samples were denatured at 100 °C and annealed slowly to room temperature. Absorbance was recorded in the forward and reverse directions at temperatures of 5 to 90 °C at a rate of 0.5 °C/min.

3.7. Photoisomerization of dU^{Az}

The *trans*-to-*cis* isomerization was performed with a UV-LED lamp (ZUV-C30H; OMRON) and a ZUV-L10H lens unit (760 mW/cm^2). The *cis*-to-*trans* isomerization was performed with a Xenon lamp (MAX-303; Asahi Spectra Co., Ltd., Tokyo, Japan) and XHQA420 optical filter. Absorbance spectra of *trans-cis* ON **7** were measured by a Shimadzu UV-Vis Spectrophotometer UV-1650PC. Conditions: ON **7** (4.0 μM), NaCl (100mM) in sodium phosphate buffer (10 mM, pH 7.0).

4. Conclusions

We have synthesized a new photoisomeric nucleoside, C5-azobenzene-modified 2'-deoxyuridine **dU^{Az}** using Sonogashira-type cross-coupling as a key step. **dU^{Az}** showed very rapid reversible *cis-trans* photoisomerization with monochromic light at the appropriate wavelength in oligodeoxynucleotide. **dU^{Az}**-modified oligodeoxynucleotide showed an interesting duplex-forming property, namely, the T_m values of both the **dU^{Az}**-modified ON/DNA and **dU^{Az}**-modified ON/RNA were higher for the cis-form than for the *trans*-form, unlike conventional azobenzene-modified ONs. Additionally, it was revealed that installation of **dU^{Az}** into oligodeoxynucleotide had little influence on the mismatch recognition ability.

Supplementary Materials

Supplementary materials can be accessed at: http://www.mdpi.com/1420-3049/19/4/5109/s1.

Acknowledgments

This work was supported by the Japan Society for the Promotion of Science (JSPS), the Ministry of Education, Culture, Sports, Science and Technology (MEXT), and theAdvanced Research for Medical Products Mining Programme of the National Institute of Biomedical Innovation (NIBIO).

Author Contributions

K.M. and S.O. designed the research. S.M. and K.M. performed the experiments and analyzed the data. S.M. was mainly responsible for writing the manuscript, with contributions from K.M. and S.O.

Conflicts of Interest

The authors declare no conflict of interest.

References

1. Kuzuya, A.; Komiyama, M. DNA origami: Fold, stick, and beyond. *Nanoscale* **2010**, *2*, 309–321.
2. Torring, T.; Voigt, N.V.; Nangreave, J.; Yan, H.; Gothelf, K.V. DNA origami: A quantum leap for self-assembly of comples structures. *Chem. Soc. Rev.* **2011**, *40*, 5636–5646.
3. Pinheiro, A.V.; Han, D.; Shin, W.M.; Yan, H. Challenges and opportunities for structural DNA nanotechnology. *Nat. Nanotechnol.* **2011**, *6*, 763–772.
4. Asanuma, H.; Ito, T.; Yoshida, T.; Liang, X.; Komiyama, M. Photoregulation of the formation and dissociation of a DNA duplex by using the *cis-trans* isomerization of azobenzene. *Angew. Chem. Int. Ed.* **1999**, *38*, 2393–2395.
5. Asanuma, H.; Liang, X.; Yoshida, T.; Komiyama, M. Photocontrol of DNA duplex formation by using azobenzene-bearing oligonucleotides. *ChemBioChem* **2001**, *2*, 39–44.
6. Beharry, A.A.; Woolley, G.A. Azobenzene photoswitches for biomolecules. *Chem. Soc. Rev.* **2011**, *40*, 4422–4437.
7. Dhammika, H.M.; Burdette, S.C. Photoisomerization in different classes of azobenzene. *Chem. Soc. Rev.* **2012**, *41*, 1809–1825.
8. Barrois, S.; Wagenknecht, H.A. Diarylehtene-modified nucleotides for switching optical properties inDNA. *Beilstein. J. Org. Chem.* **2012**, *8*, 905–914.
9. Xiao, Q.; Ranasinghe, R.T.; Tang, A.M.P.; Brown, T. Naphthalenyl- and anthracenyl-ethynyl dT analogues as base discriminating fluorescent nucleosides and intramolecular energy transfer donors in oligonucleotide probes. *Tetrahedron* **2007**, *63*, 3483–3490.
10. Franklin, R.E.; Gosling, R.G. Molecular configuration in sodium thymonucleate. *Nature* **1953**, *171*, 740–741.
11. Anderson, C.F.; Record, M.T., Jr. Salt-nucleic acid interactions. *Annu. Rev. Phys. Chem.* **1995**, *46*, 657–700.
12. Sonogashira, K.; Tohda, Y.; Hagihara, N. A convenient synthesis of acetylenes: Catalytic substitutions of acetylenic hydrogen with bromoalkenes, iodoarenes and bromopyridines. *Tetrahedron Lett.* **1975**, *16*, 4467–4470.

13. Shirai, Y.; Sasaki, T; Guerrero, J.M.; Yu, B.; Hodge, P.; Tour, J.M. Synthesis and photoisomerization of Fullerene- and oligo(phenylene ethynylene)-azobenzene derivatives. *ACS Nano* **2008**, *2*, 97–106.
14. Matharu, A.S.; Jeeva, S.; Ramanujam, P.S. Liquid crystals for holographic optical data storage. *Chem. Soc. Rev.* **2007**, *36*, 1868–1880.
15. Liang, X.; Asanuma, H.; Komiyama, M. Photoregulation of DNA triplex formation by azobenzene. *J. Am. Chem. Soc.* **2002**, *124*, 1877–1883.
16. Nishioka, H.; Liang, X.; Asanuma, H. Effect of the *ortho* modification of azobenzene on the photoregulatory efficiency of DNA hybridization and the thermal stability of its *cis* form. *Chem. Eur. J.* **2010**, *16*, 2054–2062.
17. Asanuma, H.; Yoshida, T.; Ito, T.; Komiyama, M. Photo-responsive oligonucleotides carrying azobenzene at the 2'-position of uridine. *Tetrahedron Lett.* **1999**, *40*, 7995–7998.
18. Patnaik, S.; Kumar, P.; Garg, B.S.; Gandni, R.P.; Gupta, K.C. Photomodulation of PS-modified oligonucleotides containing azobenzene substituent at pre-selected positions in phosphate backbone. *Bioorg. Med. Chem.* **2007**, *15*, 7840–7849.
19. Ogasawara, S.; Maeda, M. Straightforward and reversible photoregulation of hybridization by using a photochromic nucleoside. *Angew. Chem. Int. Ed.* **2008**, *47*, 8839–8842.
20. Nishioka, H.; Liang, X.; Kashida, H.; Asanuma, H. 2',6'-Dimethylazobenzene as an efficient and thermo-stable photoregulator for the photoregulation of DNA hybridization. *Chem. Commun.* **2007**, 4354–4356.

Sample Availability: Samples of the compounds are not available from the authors.

Organic & Biomolecular Chemistry

PAPER

View Article Online
View Journal | View Issue

Photoinduced changes in hydrogen bonding patterns of 8-thiopurine nucleobase analogues in a DNA strand†

Cite this: *Org. Biomol. Chem.*, 2014, **12**, 2468

Kunihiko Morihiro,[a,b] Tetsuya Kodama,[c] Shohei Mori[a] and Satoshi Obika*[a,b]

Received 5th December 2013,
Accepted 13th February 2014

DOI: 10.1039/c3ob42427h

www.rsc.org/obc

Hydrogen bonds (H-bonds) formed between nucleobases play an important role in the construction of various nucleic acid structures. The H-donor and H-acceptor pattern of a nucleobase is responsible for selective and correct base pair formation. Herein, we describe an 8-thioadenine nucleobase analogue and an 8-thiohypoxanthine nucleobase analogue with a photolabile 6-nitroveratryl (NV) group on the sulfur atom ($\mathbf{SA^{NV}}$ and $\mathbf{SH^{NV}}$, respectively). Light-triggered removal of the NV group causes tautomerization and a change in the H-bonding pattern of $\mathbf{SA^{NV}}$ and $\mathbf{SH^{NV}}$. This change in the H-bonding pattern has a strong effect on base recognition by 8-thiopurine nucleobase analogues. In particular, base recognition by $\mathbf{SH^{NV}}$ is clearly shifted from guanine to adenine upon photoirradiation. These results show that a photoinduced change in the H-bonding pattern is a unique strategy for manipulating nucleic acid assembly with spatiotemporal control.

Introduction

The complementarity of natural A–T and G–C base pairs in DNA is the principal mechanism for the preservation and flow of genetic information. The hydrogen-bonding (H-bonding) patterns of the four natural nucleobases play an important role in the selective and correct formation of base pairs. These H-bonding interactions can result in the formation of higher order complexes of nucleic acids, depending on the sequence. Therefore, the control of H-bonding interactions using external stimuli is important for regulating biological processes and for the possibility of developing unique DNA-based molecular machines. Various external stimuli have been used to this end; light is an ideal trigger because the timing, location, and intensity of the irradiation can be easily controlled. Among such strategies, nucleobase caging strategies involving the installation of a photolabile group are very important. Photolabile caging groups perturb the H-bonding capabilities of the nucleobases. Photoirradiation reinstates the H-bonding capabilities and allows nucleobase interaction in the "OFF to ON" direction. Nucleobase-caged nucleosides can be widely used for the photoregulation of antisense oligodeoxynucleotides (ODNs),[1,2] siRNAs,[3,4] aptamers,[5] ribozymes[6,7] and deoxyribozymes,[8,9] diagnostic ODNs,[10] DNA architectures,[11] and DNA logic gates.[12,13]

Recently, we reported the synthesis and properties of a unique light-responsive nucleobase analogue derived from 2-mercaptobenzimidazole ($\mathbf{SB^{NV}}$) (Fig. 1a).[14] $\mathbf{SB^{NV}}$ is modified with a photolabile 6-nitroveratryl (NV) group,[15] and the nitrogen at the 3-position serves as an H-acceptor (A). $\mathbf{SB^{NV}}$ can selectively form a base pair with guanine even before photoirradiation, unlike conventional caged nucleobases. Light-triggered removal of the NV group causes tautomerization of the nucleobase, and changes the role of the 3-nitrogen atom from H-A to H-donor (D). Following this change in the H-bonding pattern, base recognition by $\mathbf{SB^{NV}}$ can be shifted from guanine to adenine. We also demonstrated that a light-triggered strand exchange reaction targeting different mRNA fragment sequences could be achieved using ODNs containing $\mathbf{SB^{NV}}$. These results indicate that a photoinduced change in the H-bonding pattern of a nucleobase is a good strategy for manipulating nucleic acid assemblies in a spatially and temporally controlled manner. In this paper, to further investigate the effect of this change in H-bonding pattern of nucleobases on the base recognition ability, we designed new light-responsive nucleoside analogues bearing the NV group: 8-thioadenine and 8-thiohypoxanthine ($\mathbf{SA^{NV}}$ and $\mathbf{SH^{NV}}$, respectively;

[a]*Graduate School of Pharmaceutical Sciences, Osaka University, 1-6 Yamadaoka, Suita, Osaka 565-0871, Japan. E-mail: obika@phs.osaka-u.ac.jp; Fax: +81 6-6879-8204; Tel: +81 6-6879-8200*

[b]*National Institute of Biomedical Innovation (NIBIO), 7-6-8 Saito-Asagi, Ibaraki, Osaka 567-0085, Japan*

[c]*Graduate School of Pharmaceutical Sciences, Nagoya University, Furo-cho, Chikusa-ku, Nagoya, Aichi 464-8601, Japan*

†Electronic supplementary information (ESI) available: NMR spectra of new compounds, HPLC and MALDI-TOF MS analysis of modified ODNs, photoreaction of modified ODNs and UV melting curves for modified duplexes. See DOI: 10.1039/c3ob42427h

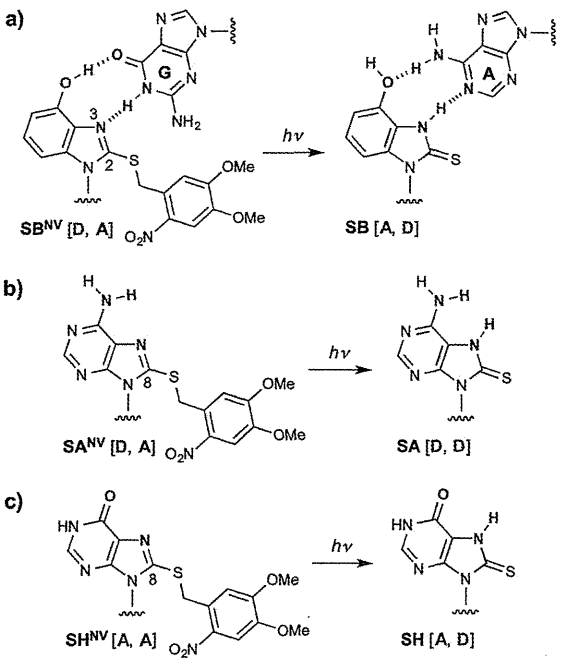

Fig. 1 (a) Change in base recognition by SB^{NV} upon photoirradiation. (b) Photoinduced changes in hydrogen bonding patterns of SA^{NV} and (c) SH^{NV}.

Fig. 1b and c). 8-Thiopurine analogues should preferentially adopt the *syn* conformation about the glycosidic bond due to steric repulsion between the C8-sulfur atom and the 4′-oxygen atom in the *anti* conformer.[16,17] SA^{NV} and SH^{NV} should also adopt the *syn* conformation and use the H-A and H-D Hoogsteen face to contact the target base. The H-bonding pattern of SA^{NV} and SH^{NV} at the Hoogsteen face would thus be changed from [D, A] to [D, D] and [A, A] to [A, D], respectively (Fig. 1). T_m evaluation of modified ODNs revealed that photoinduced changes in H-bonding patterns of 8-thiopurine nucleobase analogues have a pronounced effect on base recognition abilities.

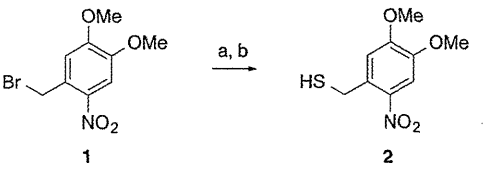

Scheme 1 Preparation of 6-nitroveratrylthiol **2**. *Reagents and conditions*: (a) KSAc, THF, rt; (b) conc. HCl aq., MeOH, 60 °C, 94% over two steps.

Results and discussion

The syntheses of the phosphoramidites bearing SA^{NV} and SH^{NV} as a nucleobase are summarized in Scheme 1. 6-Nitroveratrylthiol (2) was prepared from 6-nitroveratrylbromide (1) (Scheme 1) and subjected to reaction with 8-bromo-2′-deoxyadenosine derivative (3)[18] to afford **4** (Scheme 2). Phosphitylation at the 3′-hydroxyl group provided SA^{NV}-phosphoramidite **5**. For the preparation of SH^{NV}-phosphoramidite **9**, 8-bromoinosine (6)[19] was treated with **2** to give **7** (Scheme 3). Tritylation of the primary hydroxyl group in **7** and phosphitylation of the secondary hydroxyl group provided phosphoramidite **9**. Amidite blocks **5** and **9** were applied to an automated DNA synthesizer to incorporate SA^{NV} and SH^{NV} into ODNs. SA^{NV} and SH^{NV} were incorporated into the middle of the pyrimidine

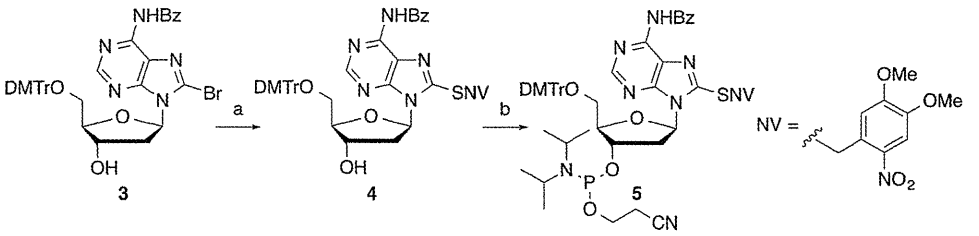

Scheme 2 Preparation of the phosphoramidites bearing SA^{NV}. *Reagents and conditions*: (a) **2**, K_2CO_3, DMF, rt, 52%; (b) $(iPr_2N)P(Cl)O(CH_2)_2CN$, iPr_2NEt, MeCN, rt, 77%.

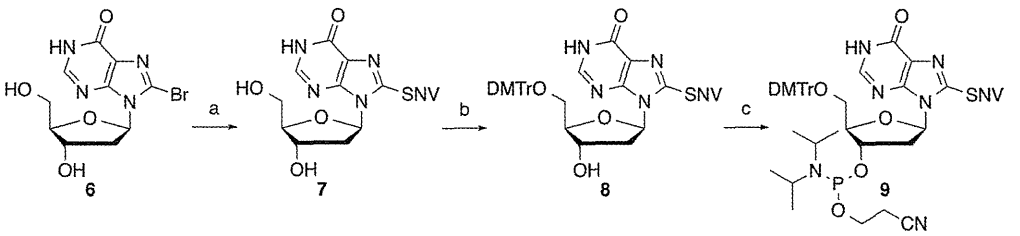

Scheme 3 Preparation of the phosphoramidites bearing SH^{NV}. *Reagents and conditions*: (a) **2**, K_2CO_3, DMF, rt, 25%; (b) DMTrCl, pyridine, rt, 85%; (c) $(iPr_2N)P(Cl)O(CH_2)_2CN$, iPr_2NEt, MeCN, rt, 74%.

10 5'-d(TCGTTT**SA**^{NV}TTGCG)-3'
11 5'-d(TCGTTT**SH**^{NV}TTGCG)-3'
12 5'-d(TCGTTTA TTGCG)-3'
13 5'-d(TCGTTTG TTGCG)-3'
14 3'-d(AGCAAAA AACGC)-5'
15 3'-d(AGCAAAG AACGC)-5'
16 3'-d(AGCAAAC AACGC)-5'
17 3'-d(AGCAAAT AACGC)-5'

Fig. 2 ODN sequences used in this study.

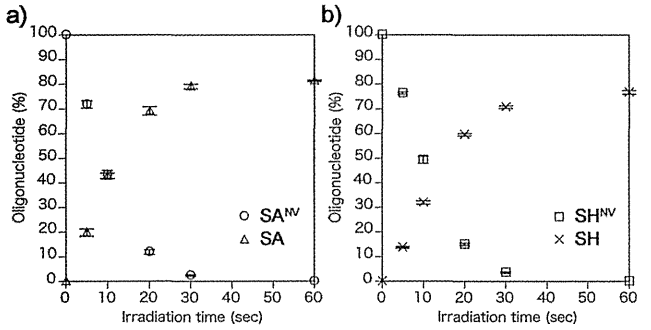

Fig. 3 Time course conversion of (a) SA^{NV} to SA in ODN **10** and (b) SH^{NV} to SH in ODN **11** by photoirradiation. Conditions: each ODN (0.1 nmol, 10 μM), sodium phosphate buffer (pH 7.2, 25 mM). Irradiation (365 nm) was performed at rt. Error bars indicate standard deviation (n = 3).

(T) strand of ODN **10** and ODN **11**. After cleavage from the resin and purification by reversed-phase (RP) HPLC, the structure of each ODN was confirmed by MALDI-TOF MS analysis. The sequence of each ODN used in this study is shown in Fig. 2.

The photoreactivity of **SA**^{NV} and **SH**^{NV} in a DNA strand was investigated by RP-HPLC analysis using ODN **10** and ODN **11**. When irradiated at 365 nm at 37 °C, ODN **10** and ODN **11** gradually disappeared. MALDI-TOF MS showed that the resulting ODNs were **SA**-/**SH**-ODNs and confirmed that the NV group of **SA**^{NV} and **SH**^{NV} was efficiently removed. Fig. 3 shows the percentage of the remaining **SA**^{NV}-/**SH**^{NV}- and resulting **SA**-/**SH**-ODNs at several irradiation time points. The photoreaction was complete within 60 s for both ODNs, and the yield of NV-removed ODNs was estimated from the HPLC peak area to be about 80%.

The effects of photoinduced changes in H-bonding patterns of **SA**^{NV} and **SH**^{NV} on their base recognition ability were examined by measuring the T_m values of DNA duplexes containing ODN **10** and ODN **11** (Table 1). ODN **10** and ODN **11** were individually hybridized to four ODNs, generating eight distinct duplexes in which each nucleobase analogue was paired with all possible natural nucleobases. For comparison, naturally matched duplexes containing the A:T and G:C base pairs in the same position were also examined. The duplex containing the **SA**^{NV}:G pair showed the highest T_m value of all the combinations of **SA**^{NV} with other nucleobases ($\Delta T_m \geqq 3$ °C). The

Table 1 T_m values of DNA duplexes[a]

5'-d(GCGTT**X**TTTGCT)-3'
3'-d(CGCAA**Y**AAACGA)-5'

Duplex	X:Y	T_m (°C) UV (−)	T_m [b] (°C) UV (+)
10:**14**	**SA**^{NV}:A	26	24
10:**15**	**SA**^{NV}:G	35	28
10:**16**	**SA**^{NV}:C	24	26
10:**17**	**SA**^{NV}:T	32	32
11:**14**	**SH**^{NV}:A	31	39
11:**15**	**SH**^{NV}:G	35	26
11:**16**	**SH**^{NV}:C	30	31
11:**17**	**SH**^{NV}:T	26	28
12:**17**	A:T	41	41
13:**16**	G:C	43	43
12:**15**	A:G (mismatch)	33	33
12:**16**	A:C (mismatch)	29	29
13:**14**	G:A (mismatch)	32	32
13:**17**	G:T (wobble)	35	35

[a] Conditions: each ODN (4.0 μM), NaCl (20 mM), sodium phosphate buffer (10 mM, pH 7.2). [b] T_m values of DNA duplexes after irradiation (365 nm) at 37 °C for 5 min.

SA^{NV}:G pair was slightly less stable than natural base pairs, and its stability was similar to the stability of the G:T wobble base pair. After photoirradiation at 365 nm for 5 min, **SA** showed the highest affinity towards thymine ($\Delta T_m \geqq 4$ °C); however, the T_m values of duplexes containing **SA** are, on the whole, low ($T_m \leqq 32$ °C). **SH**^{NV} in ODN **11** showed the highest affinity towards guanine, similar to **SA**^{NV} ($\Delta T_m \geqq 4$ °C). The T_m value of the duplex containing the **SH**^{NV}:G base pair was also slightly lower than that of natural duplexes. In contrast, after irradiation, the preferred base-pairing partner for **SH**^{NV} clearly changed to adenine ($\Delta T_m \geqq 8$ °C). Notably, the stability of **SH**:A was comparable to that of the natural A:T base pair. These results suggest that photoirradiation induces a change in base recognition by **SH**^{NV} from guanine to adenine. Fig. 4 illustrates the changes in the UV melting profiles of ODN-**11**-formed DNA duplexes and clearly indicates that the change in base recognition by **SH**^{NV} is triggered by photoirradiation.

Although further conclusive experiments such as NMR or X-ray structural analysis are needed to elucidate the precise base pair structures, the results of the T_m measurements suggest that **SA**^{NV} and **SH**^{NV} recognize guanine *via* two H bonds on the Hoogsteen face, as shown in Fig. 5. The stabilities of the **SA**^{NV} and **SH**^{NV}:G base pairs were slightly lower than that of the natural base pairs. It would appear that steric repulsion between the 8-sulfur atom in **SA**^{NV} and the 2-amino group in guanine decreases the stability of the **SA**^{NV}:G pair (Fig. 5a). This observation is consistent with previous reports showing that the base pair between 2-thiouracil and 2,6-diaminopurine is significantly destabilized because of steric hindrance.[20,21] Also, **SH**^{NV} may form a wobble pair with guanine similar to the U:G mismatch pair commonly found in RNA[22] (Fig. 5b); therefore, the **SH**^{NV}:G pair is less stable than natural base pairs. Light-induced changes in H-bonding patterns have profound effects on the base recognition abilities of 8-

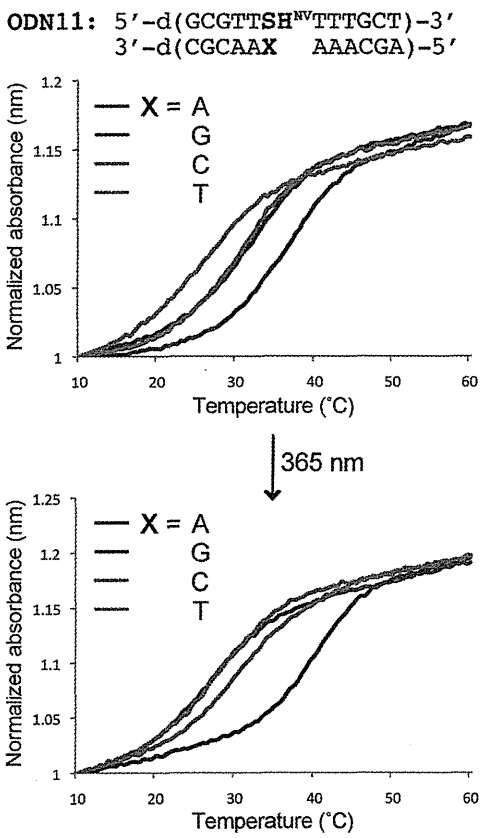

Fig. 4 Light-triggered changes in the denaturation profiles of duplexes containing ODN **11** determined by correlating the absorbance at 260 nm *vs.* temperature. Conditions as given in Table 1.

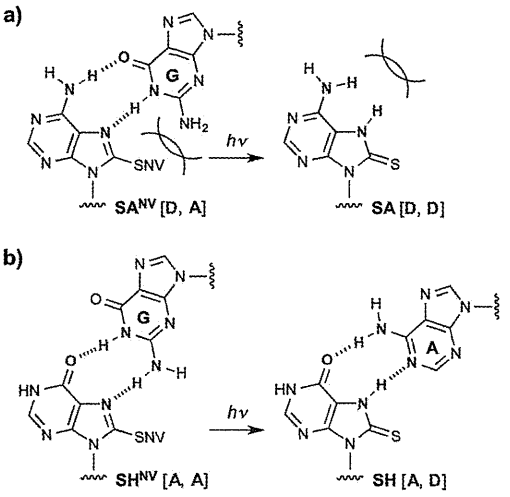

Fig. 5 Plausible change in base recognition by SA^{NV} and SH^{NV} upon photoirradiation.

thiopurine nucleobase analogues. ODN containing **SA** showed low recognition ability toward any nucleobase; this can be explained by the fact that **SA** has an H-bonding [D, D] pattern on the Hoogsteen face, but no natural nucleobase has an [A, A] pattern for base pair formation with **SA** (Fig. 5a). **SA** can interact with thymine using its Watson–Crick face in the *anti*-conformation; however, the resulting poor base-recognition-ability indicated that **SA** still adopted a *syn* conformation after photoirradiation due to the steric bulk around the 8-thio group. On the other hand, **SH** can interact with adenine using an [A, D] H-bonding pattern on the Hoogsteen face (Fig. S5†).

Conclusions

In conclusion, we have developed 8-thiopurine nucleobase analogues bearing a photolabile NV group on the sulfur atom. The H-bonding patterns of the Hoogsteen face in SA^{NV} and SH^{NV} could be changed by photoirradiation. T_m analysis indicated that light-induced changes in the H-bonding pattern profoundly influence the base recognition ability of the nucleobase in duplex DNA. In particular, base recognition by SH^{NV} is efficiently shifted from guanine to adenine upon photoirradiation. We believe that these unique light-responsive nucleobase analogues could be powerful tools for the spatio-temporal control of DNA assembly.

Experimental

General

Reagents and solvents were purchased from commercial suppliers and were used without purification unless otherwise specified. All experiments involving air- and/or moisture-sensitive compounds were carried out under an N_2 atmosphere. All reactions were monitored with analytical TLC (Merck Kieselgel 60 F254). Column chromatography was carried out using Fuji Silysia FL-100D. Physical data were measured as follows: NMR spectra were recorded on a JEOL JNM-ECS-400 spectrometer using $CDCl_3$ or DMSO-d_6 as the solvent with tetramethylsilane as an internal standard. IR spectra were recorded on a JASCO FT/IR-4200 spectrometer. Optical rotations were recorded on a JASCO P-2200 instrument. FAB mass spectra were measured on a JEOL JMS-700 mass spectrometer. MALDI-TOF mass spectra were recorded on a Bruker Daltonics Autoflex II TOF/TOF mass spectrometer.

Synthesis of the phosphoramidite-bearing SA^{NV} and SH^{NV} nucleobase analogues

6-Nitroveratrylthiol (2). To a solution of 6-nitroveratryl bromide (1.47 g, 5.36 mmol) in dry THF (54.0 mL) was added potassium thioacetate (734 mg, 6.43 mmol) and the reaction mixture was stirred for 5 h at room temperature. The solvent was removed *in vacuo* and the residue was partitioned between AcOEt and H_2O. The separated organic layer was washed with brine and then dried (Na_2SO_4) and concentrated *in vacuo*. The resulting residue (1.52 g) was dissolved in MeOH (51.0 mL), and 35% aqueous HCl (3.20 mL) was added. After being stirred for 12 h at 60 °C, the solvent was removed *in vacuo*. The residue was purified on a silica gel column eluted with hexane–AcOEt (4 : 1 to 1 : 1) to give **2** (1.15 g, 94%) as a yellow

solid; mp 86–87 °C; ^{1}H NMR (400 MHz, $CDCl_3$) δ 7.66 (1H, s), 6.86 (1H, s, H-2 or H-5), 4.03 (2H, d, J = 8.5 Hz, SCH_2Ar), 3.99 (3H, s, Ar-OCH_3), 3.95 (3H, s, Ar-OCH_3), 2.23 (1H, t, J = 8.5 Hz, SH); ^{13}C NMR (100 MHz, $CDCl_3$) δ 153.3, 147.8, 139.6, 132.0, 112.5, 108.2, 56.3, 56.2, 27.0; IR (KBr) 2577, 1520, 1273 cm^{-1}; FAB-LRMS m/z = 252 (MNa^+); FAB-HRMS calcd for $C_9H_{11}NNaO_4S$ 252.0306, found 252.0306.

6-*N*-Benzoyl-5′-*O*-(4,4′-dimethoxytrityl)-8-(6-nitroveratrylthio)-2′-deoxyadenosine (4). To a solution of 3[18] (300 mg, 0.408 mmol) in dry DMF (4.10 mL) were added K_2CO_3 (169 mg, 1.22 mmol) and 2 (103 mg, 0.449 mmol) at room temperature. After being stirred for 1 h at room temperature, the resulting mixture was partitioned between Et_2O and H_2O. The separated organic layer was washed with brine, dried (Na_2SO_4) and concentrated *in vacuo*. The resulting residue was purified on a silica gel column eluted with hexane–AcOEt (2 : 3 to 1 : 2 with 0.5% Et_3N) to give **4** (187 mg, 52%) as a yellow foam; ^{1}H NMR (400 MHz, $CDCl_3$) δ 8.93 (1H, brs, NH), 8.43 (1H, s, H-2), 8.04 (2H, d, J = 7.5 Hz), 7.64–7.16 (14H, m), 6.77–6.73 (4H, m), 6.27 (1H, t, J = 7.0 Hz, H-1′), 4.99–4.85 (3H, m, H-3′ and SCH_2Ar), 4.06 (1H, dd, J = 10.0 and 6.0 Hz, H-4′), 3.88 (3H, s, Ar-OCH_3), 3.76 (3H, s, Ar-OCH_3), 3.75 (3H, s, Ar-OCH_3), 3.71 (3H, s, Ar-OCH_3), 3.40–3.34 (3H, m, H-2′a and H-5′), 2.38 (1H, brs, OH), 2.33–2.26 (1H, m, H-2′b); ^{13}C NMR (100 MHz, $CDCl_3$) δ 164.7, 158.4, 158.4, 154.1, 153.2, 150.7, 148.4, 146.5, 144.7, 140.8, 135.9, 135.8, 133.8, 132.8, 130.0, 130.0, 128.9, 128.1, 128.0, 127.9, 127.8, 126.8, 123.7, 114.1, 113.0, 113.0, 108.0, 86.3, 85.7, 84.3, 72.8, 63.6, 56.4, 56.3, 55.2, 37.1, 33.6; IR (KBr) 1721 (C=O), 1521 (NO_2 as), 1274 (NO_2 sy) cm^{-1}; $[\alpha]_D^{22}$–64.8 (c 1.00, $CHCl_3$); FAB-LRMS m/z = 885 (MH^+); FAB-HRMS calcd for $C_{47}H_{45}N_6O_{10}S$ 885.2918, found 885.2928.

6-*N*-Benzoyl-5′-*O*-(4,4′-dimethoxytrityl)-3′-*O*-(*N*,*N*-diisopropyl-β-cyanoethylphosphoramidyl)-8-(6-nitroveratrylthio)-2′-deoxyadenosine (5). To a suspension of **4** (150 mg, 0.17 mmol) in dry MeCN (1.7 mL) were added *N*,*N*-diisopropylethylamine (0.089 mL, 0.51 mmol) and 2-cyanoethyl-*N*,*N*′-diisopropylchlorophosphoramidite (0.057 mL, 0.26 mmol) at room temperature. After being stirred for 30 min, the resulting mixture was partitioned between AcOEt and H_2O. The separated organic layer was washed with saturated aqueous $NaHCO_3$, followed by brine, then dried (Na_2SO_4) and concentrated *in vacuo*. The residue was purified on a silica gel column eluted with hexane–AcOEt (3 : 2 with 0.5% Et_3N) to give **5** (142 mg, 77%) as a yellow foam; ^{31}P NMR δ 141.4, 141.1; FAB-LRMS m/z = 1085 (MH^+); FAB-HRMS calcd for $C_{56}H_{62}N_8O_{11}PS$ 1085.3996, found 1085.4053.

8-(6-Nitroveratrylthio)-2′-deoxyinosine (7). To a solution of **6**[19] (1.65 g, 5.00 mmol) in dry DMF (50.0 mL) were added K_2CO_3 (829 mg, 6.00 mmol) and 2 (1.37 g, 6.00 mmol) at room temperature. After being stirred for 24 h at room temperature, the solvent was removed *in vacuo*. The residue was purified on a silica gel column eluted with AcOEt to AcOEt–MeOH (10 : 1) to give **7** (596 mg, 25%) as a yellow powder; ^{1}H NMR (400 MHz, DMSO-d_6) δ 12.5 (1H, brs, NH), 8.02 (1H, s), 7.68 (1H, s), 7.47 (1H, s), 6.14 (1H, t, J = 6.5 Hz, H-1′), 5.33 (1H, brs, OH), 4.91 (1H, brs, OH), 4.79 and 4.75 (each 1H, each d, J = 13.5 Hz, SCH_2Ar), 4.37 (1H, brs, H-3′), 3.86 (3H, s, Ar-OCH_3), 3.85 (3H, s, Ar-OCH_3), 3.81–3.77 (1H, m, H-4′), 3.60–3.57 (1H, m, H-5′a), 3.46–3.44 (1H, m, H-5′b), 2.98–2.91 (1H, m, H-2′a), 2.12–2.06 (1H, m, H-2′b); ^{13}C NMR (100 MHz, DMSO-d_6) δ 155.6, 152.6, 149.5, 147.9, 146.5, 145.2, 139.7, 127.4, 124.7, 115.3, 108.3, 88.0, 84.3, 70.9, 61.9, 56.1, 56.1, 37.2, 34.1; IR (KBr) 3366, 1686, 1523, 1275 cm^{-1}; FAB-LRMS m/z = 480 (MH^+); FAB-HRMS calcd for $C_{19}H_{22}N_5O_8S$ 480.1189, found 480.1207.

5′-*O*-(4,4′-Dimethoxytrityl)-8-(6-nitroveratrylthio)-2′-deoxyinosine (8). To a solution of 7 (560 mg, 1.17 mmol) in dry pyridine (12.0 mL) was added 4,4′-dimethoxytrityl chloride (474 mg, 1.40 mmol) at room temperature. After being stirred for 5 h at room temperature, the reaction was quenched by addition of MeOH. The resulting mixture was partitioned between AcOEt and H_2O. The separated organic layer was washed with saturated aqueous $NaHCO_3$, followed by brine, and then dried (Na_2SO_4) and concentrated *in vacuo*. The residue was purified on a silica gel column eluted with $CHCl_3$–MeOH (50 : 1 with 0.5% Et_3N) to give **8** (770 mg, 85%) as a yellow foam; ^{1}H NMR (400 MHz, $CDCl_3$) δ 7.70 (1H, s), 7.67 (1H, s), 7.53 (1H, s), 7.39 (1H, d, J = 7.5 Hz), 7.29–7.18 (1H, m), 6.78 (4H, dd, J = 8.5 and 3.0 Hz), 6.20 (1H, t, J = 6.5 Hz, H-1′), 4.95 and 4.91 (each 1H, each d, J = 13.5 Hz, SCH_2Ar), 4.76–4.74 (1H, m, H-3′), 4.02–3.99 (1H, m, H-4′), 3.97 (3H, s, Ar-OCH_3), 3.92 (3H, s, Ar-OCH_3), 3.77 (6H, s, 2 × Ar-OCH_3), 3.45–3.42 (1H, m, H-5′a), 3.35–3.31 (1H, m, H-5′b), 3.18–3.11 (1H, m, H-2′a), 2.30–2.23 (1H, m, H-2′b); ^{13}C NMR (100 MHz, $CDCl_3$) δ 158.4, 158.0, 153.1, 150.6, 150.0, 148.3, 144.6, 142.7, 139.9, 135.9, 130.0, 130.0, 128.2, 128.1, 127.7, 126.8, 124.9, 115.0, 113.0, 108.2, 86.3, 85.5, 84.2, 72.7, 63.8, 56.6, 56.3, 55.2, 37.5, 34.1; IR (KBr) 3007, 1678, 1519, 1276 cm^{-1}; FAB-LRMS m/z = 782 (MH^+); FAB-HRMS calcd for $C_{40}H_{40}N_5O_{10}S$ 782.2496, found 782.2531.

5′-*O*-(4,4′-Dimethoxytrityl)-3′-*O*-(*N*,*N*-diisopropyl-β-cyanoethylphosphoramidyl)-8-(6-nitroveratrylthio)-2′-deoxyinosine (9). To a solution of **8** (690 mg, 0.88 mmol) in dry MeCN (8.8 mL) was added *N*,*N*-diisopropylethylamine (0.46 mL, 2.7 mmol) and 2-cyanoethyl-*N*,*N*′-diisopropylchlorophosphoramidite (0.29 mL, 1.3 mmol) at room temperature. After being stirred for 30 min at room temperature, the resulting mixture was partitioned between AcOEt and H_2O. The separated organic layer was washed with saturated aqueous $NaHCO_3$, followed by brine, then dried (Na_2SO_4) and concentrated *in vacuo*. The residue was purified on a silica gel column eluted with hexane–AcOEt (1 : 4 with 0.5% Et_3N) to AcOEt : MeOH (10 : 1 with 0.5% Et_3N) to give **9** (600 mg, 74%) as a yellow foam; ^{31}P NMR δ 148.6, 148.4; FAB-LRMS m/z = 982 (MH^+); FAB-HRMS calcd for $C_{49}H_{57}N_7O_{11}PS$ 982.3574, found 982.3625.

Oligonucleotide synthesis

Solid-phase oligonucleotide synthesis was performed on an nS-8 Oligonucleotides Synthesizer (GeneDesign, Inc.) using commercially available reagents and phosphoramidites. The modified phosphoramidite was incorporated into the oligonucleotide with a coupling efficiency comparable to that

of commercially available phosphoramidites without any modifications to the coupling conditions. Oligonucleotides were synthesized (with trityl-off) on a 500 Å CPG solid support column (0.2 μmol scale) using 5-(bis-3,5-trifluoromethylphenyl)-1*H*-tetrazole (0.25 M in MeCN) as the activator. Cleavage from the solid support and deprotection were accomplished with concentrated ammonium hydroxide solution at 55 °C for 12 h. The crude oligonucleotides were purified on a Nap 10 column (GE Healthcare) followed by RP-HPLC on a XBridge™ OST C18 column, 2.5 μm, 10 × 50 mm (Waters) using MeCN in 0.1 M triethylammonium acetate buffer (pH 7.0). The purified oligonucleotides were quantified by UV absorbance at 260 nm and confirmed by MALDI-TOF mass spectrometry.

UV melting experiments

Melting temperatures (T_m) of the oligonucleotides were determined by measuring the change in absorbance at 260 nm as a function of temperature using a SHIMADZU UV-Vis spectrophotometer UV-1650PC equipped with a TMSPC-8 T_m analysis accessory. The samples were denatured at 100 °C and annealed slowly to room temperature. The absorbance was recorded in the forward and reverse directions between 5 and 90 °C at a rate of 0.5 °C min^{-1}. T_m values of duplexes after photoirradiation were measured using samples irradiated (365 nm) at 37 °C.

Photoirradiation reaction

Photoirradiation of oligonucleotides was performed in sodium phosphate buffer (pH 7.2) at 37 °C for 5 minutes using an OMRON UV-LED lamp ZUV-C30H as the light source (365 nm) and a ZUV-L10H as the lens unit (760 mW cm^{-2}). Analyses of the photoproducts were carried out without further purification.

Acknowledgements

This work was supported by the Japan Society for the Promotion of Science (JSPS), the Ministry of Education, Culture, Sports, Science and Technology (MEXT), and the Advanced Research for Medical Products Mining Programme of the National Institute of Biomedical Innovation (NIBIO), Japan.

Notes and references

1 D. D. Young, H. Lusic, M. O. Lively, J. A. Yoder and A. Deiters, *ChemBioChem*, 2008, **9**, 2937.
2 D. D. Young, M. O. Lively and A. Deiters, *J. Am. Chem. Soc.*, 2010, **132**, 6183.
3 V. Mikat and A. Heckel, *RNA*, 2007, **13**, 2341.
4 J. M. Govan, D. D. Young, H. Lusic, Q. Liu, M. O. Lively and A. Deiters, *Nucleic Acids Res.*, 2013, **41**, 10518.
5 A. Heckel and G. Mayer, *J. Am. Chem. Soc.*, 2005, **127**, 822.
6 C. Höbartner and S. K. Silverman, *Angew. Chem., Int. Ed.*, 2005, **44**, 7305.
7 A. Nierth, M. Singer and A. Jäschke, *Chem. Commun.*, 2010, **46**, 7975.
8 H. Lusic, D. D. Young, M. O. Lively and A. Deiters, *Org. Lett.*, 2007, **9**, 1903.
9 H. Lusic, M. O. Lively and A. Deiters, *Mol. BioSyst.*, 2008, **4**, 508.
10 K. B. Joshi, A. Vlachos, V. Mikat, T. Deller and A. Heckel, *Chem. Commun.*, 2012, **48**, 2746.
11 T. L. Schmidt, M. B. Koeppel, J. Thevarpadam, D. P. N. Goncalves and A. Heckel, *Small*, 2011, **7**, 2163.
12 A. Prokup, J. Hemphill and A. Deiters, *J. Am. Chem. Soc.*, 2012, **134**, 3810.
13 J. Hemphill and A. Deiters, *J. Am. Chem. Soc.*, 2013, **135**, 10512.
14 K. Morihiro, T. Kodama, R. Waki and S. Obika, *Chem. Sci.*, 2014, **5**, 744.
15 A. Patchornik, B. Amit and R. B. Woodward, *J. Am. Chem. Soc.*, 1970, **92**, 6333.
16 M. L. Hamm, R. Cholera, C. L. Hoey and T. J. Gill, *Org. Lett.*, 2004, **6**, 3817.
17 K. Miyata, R. Tamamushi, H. Tsunoda, A. Ohkubo, K. Seio and M. Sekine, *Org. Lett.*, 2009, **11**, 605–608.
18 T. P. Prakash, R. K. Kumer and K. N. Ganesh, *Tetrahedron*, 1993, **49**, 4035.
19 R. E. Holmes and R. K. Robins, *J. Am. Chem. Soc.*, 1964, **86**, 1242.
20 I. V. Kutyavin, R. L. Rhinehart, E. A. Lukhtanov, V. V. Gorn, R. B. Meyer Jr. and H. B. Gamper Jr., *Biochemistry*, 1996, **35**, 11170.
21 J. Lohse, O. Dahl and P. E. Nielsen, *Proc. Natl. Acad. Sci. U. S. A.*, 1999, **96**, 11804.
22 G. Varani and W. H. McClain, *EMBO Rep.*, 2000, **1**, 18.

8174–8187 *Nucleic Acids Research, 2014, Vol. 42, No. 12* *Published online 16 June 2014*
doi: 10.1093/nar/gku512

Design and evaluation of locked nucleic acid-based splice-switching oligonucleotides *in vitro*

Takenori Shimo[1,†], Keisuke Tachibana[1,†], Kiwamu Saito[1], Tokuyuki Yoshida[1,2], Erisa Tomita[3], Reiko Waki[1], Tsuyoshi Yamamoto[1], Takefumi Doi[1], Takao Inoue[1,2], Junji Kawakami[3,4] and Satoshi Obika[1,*]

[1]Graduate School of Pharmaceutical Sciences, Osaka University, 1–6, Yamadaoka, Suita, Osaka, 565–0871, Japan, [2]Division of Cellular and Gene Therapy Products, National Institute of Health Sciences, 1–18–1 Kamiyoga, Setagaya-ku, Tokyo 158–8501, Japan, [3]Department of Nanobiochemistry, FIRST, Konan University, 7–1–20 Minatojima-minamimachi, Chuo-ku, Kobe 650–0047, Japan and [4]Frontier Institute for Biomolecular Engineering Research (FIBER), Konan University, 7–1–20 Minatojima-minamimachi, Chuo-ku, Kobe 650–0047, Japan

Received October 19, 2013; Revised May 22, 2014; Accepted May 23, 2014

ABSTRACT

Antisense-mediated modulation of pre-mRNA splicing is an attractive therapeutic strategy for genetic diseases. Currently, there are few examples of modulation of pre-mRNA splicing using locked nucleic acid (LNA) antisense oligonucleotides, and, in particular, no systematic study has addressed the optimal design of LNA-based splice-switching oligonucleotides (LNA SSOs). Here, we designed a series of LNA SSOs complementary to the human dystrophin exon 58 sequence and evaluated their ability to induce exon skipping *in vitro* using reverse transcription-polymerase chain reaction. We demonstrated that the number of LNAs in the SSO sequence and the melting temperature of the SSOs play important roles in inducing exon skipping and seem to be key factors for designing efficient LNA SSOs. LNA SSO length was an important determinant of activity: a 13-mer with six LNA modifications had the highest efficacy, and a 7-mer was the minimal length required to induce exon skipping. Evaluation of exon skipping activity using mismatched LNA/DNA mixmers revealed that 9-mer LNA SSO allowed a better mismatch discrimination. LNA SSOs also induced exon skipping of endogenous human dystrophin in primary human skeletal muscle cells. Taken together, our findings indicate that LNA SSOs are powerful tools for modulating pre-mRNA splicing.

INTRODUCTION

Alternative pre-mRNA splicing is an essential system for gene expression in eukaryotes that allows the production of various types of proteins from a limited set of genes (1). However, mutations in splice sites cause mis-splicing, which is followed by genetic diseases (2,3,4). To correct these splicing errors, exon skipping by using antisense oligonucleotides (AONs) has been suggested (5,6). These splice-switching oligonucleotides (SSOs) bind to target sequences in pre-mRNA and prevent the interaction of various splicing modulators (7). Thus, SSOs are able to modulate pre-mRNA splicing and repair defective RNA without inducing the RNase H-mediated cleavage of mRNA (8,9).

To enhance the *in vivo* activity of AONs, many artificial nucleic acids have been synthesized to improve nuclease resistance, binding properties, RNase H activity and serum stability (10,11). Locked nucleic acid (LNA) (also known as 2'-*O*,4'-*C*-methylene-bridged nucleic acid (2',4'-BNA)) is an artificial nucleic acid derivative that was synthesized by us and by Wengel's group independently in the late 1990s (12,13). LNA contains a methylene bridge connecting the 2'-*O* with the 4'-*C* position in the furanose ring, which enables it to form a strictly *N*-type conformation that offers high binding affinity against complementary RNA (14,15,16). LNA also presents enzyme resistance, similar to other nucleic acid derivatives. Given these features, LNA can be used for various gene silencing techniques, such as antisense, short interfering RNA, blocking of microRNA and triplex-forming oligonucleotides. Previous studies also showed that LNA could be used in SSOs (17,18,19,20), and LNA-based SSOs (LNA SSOs) have been shown to be functional *in vivo* in mouse models (21,22).

Recently, SSOs based on 2'-*O*-methyl RNA (2'-OMe) with a full-length phosphorothioate (PS) backbone,

*To whom correspondence should be addressed. Tel: +81 6 6879 8200; Fax: +81 6 6879 8204; Email: obika@phs.osaka-u.ac.jp
†The authors wish it to be known that, in their opinion, the first two authors should be regarded as Joint First Authors.

phosphorodiamidate morpholino oligomer or 2'-*O*,4'-*C*-ethylene-bridged nucleic acids have been applied to clinical trials for the treatment of genetic diseases, particularly Duchenne muscular dystrophy (DMD) (23,24,25,26,27,28). DMD is a severe muscle-weakening disease that arises from mutations in dystrophin, which links the cytoskeleton to the extracellular matrix of muscle fibers. Mutations in the dystrophin gene lead to premature termination of translation and prevent the synthesis of a functional gene product. SSO-mediated exon skipping in dystrophin pre-mRNA can restore the reading frame and allow the expression of a truncated but functional dystrophin similar to that found in Becker muscular dystrophy patients, who have relatively milder symptoms (29). Thus, modulation of splicing using SSOs is an attractive strategy for the treatment of genetic diseases, such as DMD. However, relatively few studies have used LNA SSOs compared to those using SSOs based on other chemistries.

Methods for designing effective SSOs have recently been developed and provide insight into factors that are critical for SSO activity, including the melting temperature (T_m), guanine-cytosine content and secondary structures or sequence motifs that correspond to splicing signals of the target RNA (30,31). Because LNA oligonucleotides possess high binding affinity to complementary RNA, the SSOs that incorporate LNA are considered as promising tools for inducing exon skipping. However, no systematic study has addressed the optimal design of LNA SSOs. Therefore, in this study, we designed a series of LNA SSOs complementary to the human dystrophin exon 58 sequence, and evaluated their ability to induce exon skipping using reverse transcription-polymerase chain reaction (RT-PCR) and a minigene reporter encompassing exons 57–59 of the human dystrophin gene.

MATERIALS AND METHODS

Synthesis of oligonucleotides

All SSOs used in this study are shown in Supplementary Tables S1–S9. Two types of modification, LNA and 2'-OMe, were incorporated into the SSO sequences, in which the phosphodiester linkages were completely replaced by PS linkages (Figure 1). All SSOs were designed to have sequences complementary to human dystrophin gene and were synthesized and purified by Gene Design Inc. (Osaka, Japan).

Plasmid construction

The reporter construct was generated using standard cloning techniques published in a previous study (32). A FLAG (DYKDDDDK)-coding oligonucleotide was constructed by annealing the forward oligonucleotide 5'-AGCTTACCATGGATTACAAGGACGACGAC GACAAGGGGGTAC-3' (including HindIII and KpnI sites, underlined) and reverse oligonucleotide 5'-CCCCTTGTCGTCGTCGTCCTTGTAATCCATGGTA-3'. The annealed oligonucleotide was cloned into the HindIII-KpnI sites of the pcDNA5/FRT vector (Invitrogen, Carlsbad, CA, USA) (termed pcDNA5/FRT-FLAG). The EGFP fragment was obtained by PCR using the forward primer 5'-CCCGGGTGTGAGCAAGGGCGAGGAGCTGT-3' (including a SmaI site, underlined) and reverse primer 5'-ATAGGGCCCTTACTTGTACAGCTCGTCCAT-3' (including an ApaI site, underlined). The obtained EGFP fragment was cloned into the EcoRV-ApaI sites of pcDNA5/FRT-FLAG (termed pcDNA5/FRT-FLAG-EGFP). The DsRed fragment was obtained by PCR from the pDsRed-Express-N1 vector (Clontech, Mountain View, CA, USA) using the forward primer 5'-ATATGGATCCAACCGGTGTGGCC TCCTCCGAGGACGTCA-3' (including BamHI and AgeI sites, underlined) and reverse primer 5'-CGGTCTACAGGAACAGGTGGTGGC-3'. The obtained DsRed fragment was cloned into the BamHI-SmaI sites of the pcDNA5/FRT-FLAG-EGFP vector (termed pcDNA5/FRT-FLAG-DsRed-EGFP). A nuclear localization signal (NLS) was constructed by annealing the forward oligonucleotide 5'-ATGCCCCAAAAAAAAA ACGCAAAGTGGAGGACCCAAAGGTACCAAAG-3' (including a KpnI site, underlined) and reverse oligonucleotide 5'-GATCCTTTGGTACCTTTGGGTCCTCCAC TTTGCGTTTTTTTTTTGGGGCATGTAC-3'. The annealing oligonucleotide was cloned into the KpnI-BamHI sites of pcDNA5/FRT-FLAG-DsRed-EGFP (termed pcDNA5/FRT-FLAG-NLS-DsRed-EGFP).

A human dystrophin minigene containing exons 57–59 was isolated as follows. Because the intron 57 sequence consists of 17 684 bp and is thus too long to insert into a plasmid, we designed a human dystrophin minigene by removing the sequence of intron 57 from position +207 to +17 486. Thus, exon 57, together with a short flanking intronic sequence, was obtained by PCR from the HepG2 genome using the forward primer 5'-AACGGTACCAACGCTGCTGTTCTTTTTCA-3' (including a KpnI site, underlined) and reverse primer 5'-GTGTTTGTAATGGACGATTTCTTAAAGGGTATT-3'. Another fragment containing a short 3' sequence of intron 57 to exon 59 was also obtained by PCR using the forward primer 5'-AAATCGTCCATTACAAACACAGCGCTTTCC-3' and reverse primer 5'-AGACCGGTACTCCTCAGCCTGCTTTCGTA-3' (including an AgeI site, underlined). These two fragments were mixed, and a second round of PCR was performed. Finally, after the second round of PCR, the newly synthesized full-length PCR product was cloned into the KpnI-AgeI sites of the pcDNA5/FRT-FLAG-NLS-DsRed-EGFP vector to generate a dystrophin reporter minigene (termed pcDNA5/FRT-FLAG-NLS-DMD-Exon57_58_59(short-Intron57)-DsRed-EGFP). All constructs were verified by sequencing.

Generation of a stable cell line

Flp-In 293 cells (Invitrogen) were cultured in Dulbecco's modified Eagle Medium (DMEM) (Nacalai Tesque, Kyoto, Japan) containing 10% fetal bovine serum (FBS) (Biowest, Nuaillé, France), 100 units/ml penicillin and 100 μg/ml streptomycin (Nacalai Tesque) and maintained in a 5% CO_2 incubator at 37°C. Flp-In 293 cells were

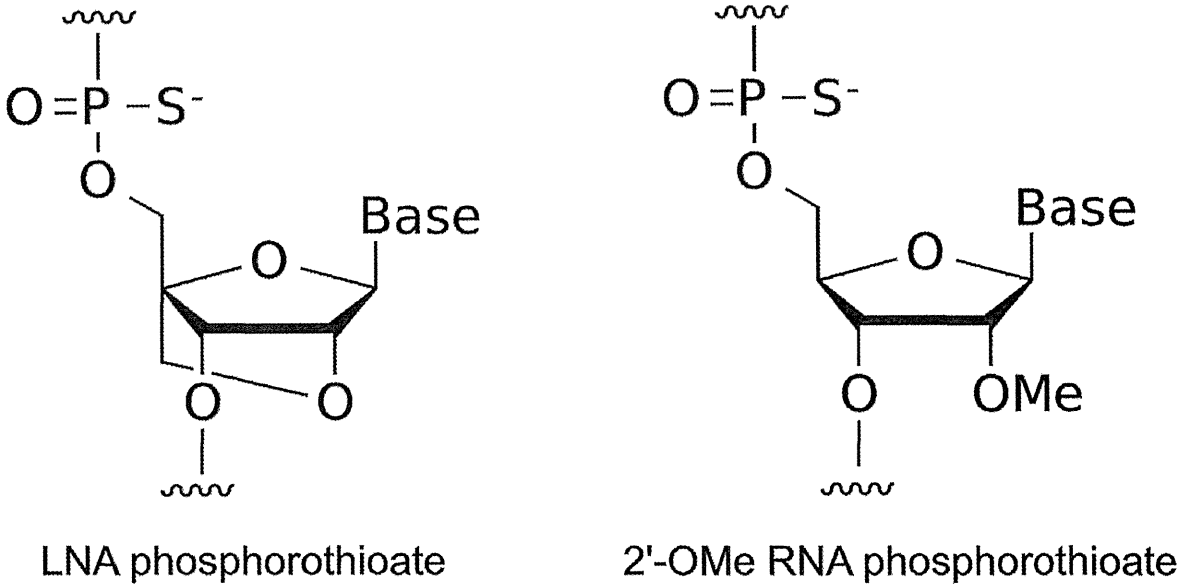

Figure 1. Structures of the building blocks for SSOs. PS LNA and PS 2'-OMe RNA.

co-transfected with pcDNA5/FRT-FLAG-NLS-DMD-Exon57_58_59(short-Intron57)-DsRed-EGFP and pOG44 (the flp recombinase expression plasmid) (Invitrogen). Stable cell lines were selected by 50 μg/ml hygromycin B (Invitrogen).

SSOs transfection

Stable cell lines were seeded one day before transfection at a density of 8.0×10^4 cells/well on 24-well plates. At 30%–40% confluence, SSOs were transfected into cells by using Lipofectamine 2000 (Invitrogen) according to the manufacturer's instructions. After 24 h, the cells were harvested.

RNA isolation and cDNA synthesis

Total RNA samples were isolated from the cells using the QuickGene 800 and QuickGene RNA cultured cell kit S (KURABO, Osaka, Japan) according to the manufacturer's instructions. First-strand cDNA was synthesized from 150 ng of the total RNA of each cell sample using the ReverTra Ace qPCR RT Master Mix (TOYOBO, Osaka, Japan) according to the manufacturer's instructions.

Primary myoblast cell culture, SSO transfection and RNA isolation

Primary human skeletal muscle myoblasts (HSMM) derived from healthy Caucasian donor (female aged 17 years) were purchased from Lonza (Walkersville, MD, USA). HSMM cells were cultured in SkBM-2 basal medium (Lonza) supplemented with 10% FBS, epidermal growth factor (EGF), dexamethasone, L-glutamine, gentamycin sulfate and amphotericin B (SingleQuots, Lonza) and maintained in a 5% CO_2 incubator at 37°C. For SSO transfection, cells were seeded 2 days before transfection at a density of 1.0×10^5 cells/well on 24-well collagen type I coated plates. After 24 h, cells were differentiated by changing the growth medium to differentiation medium (DMEM/F-12 (Life Technologies, Carlsbad, CA, USA) containing 2% horse serum (Life Technologies) and antibiotic-antimycotic solution (100 units/ml penicillin, 100 μg/ml streptomycin, 0.25 μg/ml amphotericin B) (Life Technologies)) for 24 h. Cells were transfected with 500 nM SSOs using Lipofectamine 2000 according to the manufacturer's instructions. Twenty-four hours after transfection, total RNA samples were isolated from the cells using the QuickGene 800 and QuickGene RNA cultured cell kit S according to the manufacturer's instructions. First-strand cDNA was synthesized from 50 ng of the total RNA of each cell sample using the ReverTra Ace qPCR RT Master Mix according to the manufacturer's instructions.

RT-PCR analysis

The cDNA was used as a template for individual PCR reactions using specific primer sets (Supplementary Table S10), which were designed using the Primer3 program written by the Whitehead Institute (33). PCR reactions were conducted using KOD FX Neo DNA polymerase (TOYOBO), and the PCR products were analyzed on a 2% agarose gel stained with ethidium bromide, with specific bands purified for sequence analysis. The intensity of each band was quantified by using ImageJ software (National Institutes of Health; freeware from http://rsb.info.nih.gov/ij/) and normalized according to the nucleotide composition. The exon skipping percentage was calculated as the amount of exon 58-skipped transcript relative to the total amount of the exon 58-skipped and full-length transcripts (34). Glyceraldehyde-3-phosphate dehydrogenase (GAPDH) was used as an internal control.